Inorg. Chem. **2005**, *44*, 1505–1510

Deprotonation Reactions of Zirconium and Hafnium Amide Complexes H_2N–$M[N(SiMe_3)_2]_3$ and Subsequent Silyl Migration from Amide $–N(SiMe_3)_2$ to Imide $=NH$ Ligands

Xianghua Yu and Zi-Ling Xue*

Department of Chemistry, The University of Tennessee, Knoxville, Tennessee 37996-1600

Received October 19, 2004

Ammonolysis of previously reported $Cl–M[N(SiMe_3)_2]_3$ (M = Zr, **1a**; Hf, **1b**) leads to the formation of peramides $H_2N–M[N(SiMe_3)_2]_3$ (M = Zr, **2a**; Hf, **2b**) which upon deprotonation by $LiN(SiMe_3)_2$ or $Li(THF)_3SiPh_2Bu^t$ yields imides $Li^+(THF)_n\{HN^––M[N(SiMe_3)_2]_3\}$ (M = Zr, **3a**; Hf, **3b**). One $–SiMe_3$ group in **3a**–**b** undergoes silyl migration from a $–N(SiMe_3)_2$ ligand to the imide $=NH$ ligand to give $Li^+(THF)_2\{Me_3SiN^––M[NH(SiMe_3)][N(SiMe_3)_2]_2\}$ (M = Zr, **4a**; Hf, **4b**) containing an imide $=N(SiMe_3)$ ligand. The kinetics of the **3a** → **4a** conversion was investigated between 290 and 315 K and was first-order with respect to **3a**. The activation parameters for this silyl migration are $\Delta H^‡ = 13.3(1.3)$ kcal/mol and $\Delta S^‡ = –34(3)$ eu in solutions of **3a** (in toluene-d_8 with 1.07 M THF) prepared in situ. THF in the mixed solvent promoted the **3a** → **4a** reaction. The effect of THF on the rate constants of the conversion has been studied, and the kinetics of the reaction was 3.4(0.6)th order with respect to THF. Crystal and molecular structures of $H_2N–Zr[N(SiMe_3)_2]_3$ (**2a**) and **4a**–**b** have been determined.

Metal amide complexes are of intense current interest as precursors to metal nitrides, M−Si−N ternary solids, and metal oxides in molecular approaches to microelectronic thin film materials.[1] Ammonolysis between NH_3 and $M(NR_2)_n$ plays a critical role in the preparation of nitrides and M−Si−N ternary solids.[2] In addition, ammonolysis between NH_3 and MCl_n has also been used to make metal nitrides.[2a−c] Metal amide ($-NH_2$), imide ($=NH$), and nitride ($\equiv N$) are believed to be among the intermediates. Only a few isolated early-transition-metal complexes containing $-NH_2$ ligands have been reported,[3] and they usually have ancillary ligands such as Cp* (C_5Me_5).[3b,c]

Silyl migration is well known largely because of the high migratory aptitude of silyls in comparison to alkyls.[4] There are relatively few reported cases of intramolecular $-SiMe_3$ migration between two N atoms as N−Si bonds are usually strong, and these reported cases mainly involve 1,2 anionic migration.[5] 1,3-Anionic silyl migration between two N atoms is rare.[6] To our knowledge, no silyl migration between N atoms in transition-metal complexes has been reported. Peramide complexes $H_2N-M[N(SiMe_3)_2]_3$ (M = Zr, **2a**; Hf, **2b**) containing $-NH_2$ ligands have been prepared through

* Author to whom correspondence should be addressed. E-mail: xue@utk.edu.

(1) (a) Toth, L. E. In *Transition Metal Carbides and Nitrides*; Margrave, J. L., Ed.; Academic Press: New York, 1971; Vol. 7. (b) Fix, R.; Gordon, R. G.; Hoffman, D. M. *Chem. Mater.* **1991**, *3*, 1138. (c) Fix, R.; Gordon, R. G.; Hoffman, D. M. *Chem. Mater.* **1993**, *5*, 614.

(2) (a) Hoffman, D. M. *Polyhedron* **1994**, *13*, 1169. (b) Dubois, L. H. *Polyhedron* **1994**, *13*, 1329. (c) Baxter, D. V.; Chisholm, M. H.; Gama, G. J.; DiStasi, V. F.; Hector, A. L.; Parkin, I. P. *Chem. Mater.* **1996**, *8*, 1222. (d) Fix, R. M.; Gordon, R. G.; Hoffman, D. M. *J. Am. Chem. Soc.* **1990**, *112*, 7833.

(3) (a) Banaszak Holl, M. M.; Wolczanski, P. T. *J. Am. Chem. Soc.* **1992**, *114*, 3854. (b) Bai, G.; Vidovic, D.; Roesky, H. W.; Magull, J. *Polyhedron* **2004**, *23*, 1125. (c) Abarca, A.; Gomez-Sal, P.; Martin, A.; Mena, M.; Poblet, J. M.; Yelamos, C. *Inorg. Chem.* **2000**, *39*, 642.

(4) (a) Brook, A. G.; Bassindale, A. R. In *Rearrangements in Ground and Excited States;* Mayo, P., Ed.; Academic Press: New York, 1980; Vol. 2, Chapter 9, p 149. (b) Kira, M.; Iwamoto, T. In *The Chemistry of Organic Silicon Compounds*; Rappoport, Z., Apeloig, Y., Eds.; Wiley: New York, 2001; Vol. 3, Chapter 16, pp 853−948.

(5) (a) West, R.; Bichlmeir, B. *J. Am. Chem. Soc.* **1972**, *94*, 1649. (b) Bailey, R. E.; West, R. *J. Am. Chem. Soc.* **1964**, *86*, 5369. (c) West, R.; Ishikawa, M.; Bailey, R. E. *J. Am. Chem. Soc.* **1966**, *88*, 4648. (d) West, R.; Ishikawa, M.; Bailey, R. E. *J. Am. Chem. Soc.* **1967**, *89*, 4068. (e) West, R.; Ishikawa, M.; Bailey, R. E. *J. Am. Chem. Soc.* **1967**, *89*, 4072. (f) West, R.; Ishikawa, M. *J. Am. Chem. Soc.* **1967**, *89*, 4981.

(6) (a) Neugcbauer, P.; Jaschke, B.; Klingebiel, U. In *The Chemistry of Organic Silicon Compounds*; Rappoport, Z., Apeloig, Y., Eds.; Wiley: New York, 2001; Vol. 3, Chapter 6, pp 429−467. (b) Bush, R. P.; Lloyd, N. C.; Pearce, C. A. *Chem. Commun.* **1968**, 1191. (c) Breed, L. W. *Inorg. Chem.* **1968**, *7*, 1940. (d) Fink, W. *Helv. Chim. Acta* **1969**, *52*, 2261. (e) Klingebiel, U.; Noltemeyer, M.; Rakebrandt, H.-J. *Z. Anorg. Allg. Chem.* **1997**, *623*, 281. (f) Dippel, K.; Werner, E.; Klingebiel, U. *Phosphorus, Sulfur Silicon* **1992**, *64*, 15.

10.1021/ic0485413 CCC: $30.25
Published on Web 02/15/2005

Scheme 1. Preparation of **2a**−**b** and **4a**−**b** (*k*: Rate Constant of the **3a** → **4a** Conversion)

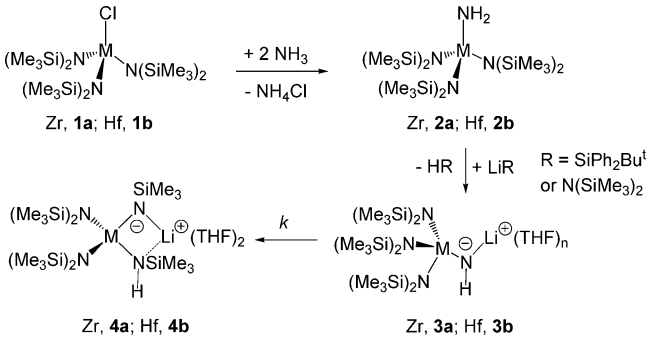

ammonolysis of Cl−M[N(SiMe$_3$)$_2$]$_3$ (M = Zr, **1a**; Hf, **1b**, Scheme 1). Upon deprotonation of H$_2$N−M[N(SiMe$_3$)$_2$]$_3$ (M = Zr, **2a**; Hf, **2b**) to give Li$^+$(THF)$_n${HN$^-$−M[N(SiMe$_3$)$_2$]$_3$} (M = Zr, **3a**; Hf, **3b**) containing an imide ═NH ligand, 1,3-anionic silyl migration between −N(SiMe$_3$)$_2$ and the imide ligand occurs to give Li$^+$(THF)$_2${Me$_3$SiN$^-$−M[NH(SiMe$_3$)][N(SiMe$_3$)$_2$]$_2$} (M = Zr, **4a**; Hf, **4b**) containing a new imide ligand ═N(SiMe$_3$) (Scheme 1). Kinetics of the **3a** → **4a** conversion and the effect of THF on the rate of the reaction have also been investigated. These studies are reported here.

Experimental Section

All manipulations were performed under a dry nitrogen atmosphere with the use of either a drybox or standard Schlenk techniques. Solvents were purified by distillation from potassium/benzophenone ketyl. Benzene-d_6 and toluene-d_8 were dried over activated molecular sieves and stored under N$_2$. ZrCl$_4$ (Strem) and HfCl$_4$ (Strem) were freshly sublimed under vacuum. Li(THF)$_3$SiPh$_2$Bu^t was prepared by the literature procedure.[7] LiN(SiMe$_3$)$_2$ (Aldrich) was used as received. NH$_3$ was dried through two columns of KOH pellets and one column of Drierite (W. A. Hammond Drierite Company, Ohio) before it was used. ^{1}H and ^{13}C{^{1}H} NMR spectra were recorded on a Bruker AMX-400 spectrometer and referenced to solvent (residual protons in the ^{1}H spectra). FT-IR spectra were recorded on an MB-100 spectrometer (Bomem, Inc., Quebec, Canada). Elemental analyses were performed by Complete Analysis Laboratories Inc., Parsippany, New Jersey.

For the kinetic studies of the **3a** → **4a** conversion and the effect of THF, the first-order rate constants *k* were obtained from at least two separate experiments at a given temperature and a concentration of THF, and their averages are listed. The estimated uncertainty in the temperature measurements for an NMR probe was 1 K. The enthalpy ($\Delta H^{\ddagger}$), entropy ($\Delta S^{\ddagger}$), and the order of THF (*m*) on rate constants were calculated from an unweighted nonlinear least-squares procedure contained in the SigmaPlot Scientific Graph System. The uncertainties in $\Delta H^{\ddagger}$ and $\Delta S^{\ddagger}$ were computed from the error propagation formulas developed by Girolami and coworkers.[8] The uncertainties in *m* was calculated from the following error propagation formulas (eq 1):[9]

$$(\sigma m)^2 = \frac{2 \times (\Delta \ln k)^2}{(\Delta \ln C_{\mathrm{THF}})^4} \times \left(\frac{\sigma C_{\mathrm{THF}}}{C_{\mathrm{THF}}}\right)^2 + \frac{2}{(\Delta \ln C_{\mathrm{THF}})^2} \times \left(\frac{\sigma k}{k}\right)^2$$

$$\Delta \ln C_{\mathrm{THF}} = (\ln C_{\mathrm{THFmax}} - \ln C_{\mathrm{THFmin}}) \qquad (1)$$

Preparation of H$_2$N−M[N(SiMe$_3$)$_2$]$_3$ (M = Zr, 2a; Hf, 2b). A slurry of MCl$_4$ (3.00 g of ZrCl$_4$, 12.9 mmol, or 4.00 g of HfCl$_4$, 12.5 mmol) in THF was treated with 3 equiv of LiN(SiMe$_3$)$_2$ (6.46 g, 38.6 mmol for ZrCl$_4$ or 6.27 g, 37.5 mmol for HfCl$_4$) in THF dropwise at −50 °C. The solution was warmed to room temperature and stirred overnight. All volatiles were removed in vacuo, and the solid was extracted with warm hexanes (55 °C). Excess dried NH$_3$ was then bubbled through the light-yellow solution for 40 min. All volatiles were then removed in vacuo, and the solid was extracted with pentane. The solution was then concentrated to ca. 2.5 mL and kept in a freezer at −36 °C overnight to give colorless crystals of **2a** (2.58 g, 4.38 mmol, 34.1%) or **2b** (2.60 g, 3.85 mmol, 30.8%).

For **2a**: ^{1}H NMR (benzene-d_6, 400.0 MHz, 23 °C) δ 4.26 [t, 2H, NH_2, $^1J(^{14}\mathrm{N}-\mathrm{H})$ = 45.6 Hz], 0.36 [s, 54H, N(SiMe_3)$_2$]; ^{13}C{^{1}H} NMR (benzene-d_6, 100.6 MHz, 23 °C) δ 6.08 [N(SiMe_3)$_2$]. FT-IR (Nujol): 3342 (m, N−H), 2950 (s), 2908 (m), 1504 (w), 1403 (m), 1250 (s), and 897 (s) cm^{-1}. Anal. calcd for C$_{18}$H$_{56}$N$_4$Si$_6$Zr: C, 36.74; H, 9.59. Found: C, 36.49; H, 9.48.

For **2b**: ^{1}H NMR (benzene-d_6, 400.0 MHz, 23 °C) δ 3.67 [t, 2H, NH_2, $^1J(^{14}\mathrm{N}-\mathrm{H})$ = 46.0 Hz], 0.36 [s, 54H, N(SiMe_3)$_2$]; ^{13}C{^{1}H} NMR (benzene-d_6, 100.6 MHz, 23 °C) δ 6.26 [N(SiMe_3)$_2$]. FT-IR (Nujol): 3364 (m, N−H), 2957 (s), 2898 (m), 1509 (m), 1398 (w), 1247 (s), and 844 (s) cm^{-1}. Anal. calcd for C$_{18}$H$_{56}$N$_4$Si$_6$Hf: C, 32.00; H, 8.35. Found: C, 31.79; H, 8.29.

Observation of Li(THF)$_n${HN−M[N(SiMe$_3$)$_2$]$_3$} (M = Zr, 3a; Hf, 3b) and Preparation of Li(THF)$_2${Me$_3$SiN−M[NH(SiMe$_3$)][N(SiMe$_3$)$_2$]$_2$} (M = Zr, 4a; Hf, 4b). A mixture of H$_2$N−M[N(SiMe$_3$)$_2$]$_3$ (0.535 g, 0.909 mmol for **2a** or 0.610 g, 0.903 mmol for **2b**) and LiN(SiMe$_3$)$_2$ (0.152 g, 9.08 mmol for **2a** or 0.151 g, 9.02 mmol for **2b**) was treated with THF (40 mL for **2a** or 30 mL for **2b**). An immediate formation of unstable Li(THF)$_n${HN−M[N(SiMe$_3$)$_2$]$_3$} (M = Zr, **3a**; Hf, **3b**) was observed, which converted to **4a** or **4b**. All volatiles were then removed in vacuo after the solution was stirred at room temperature overnight. The resulting solid was extracted by pentane, and the extract was concentrated and kept in a freezer at −36 °C overnight to give colorless crystals of **4a** (0.372 g, 0.504 mmol, 55.4%) or **4b** (0.346 g, 0.419 mmol, 46.4%). Reactions of H$_2$N−M[N(SiMe$_3$)$_2$]$_3$ (M = Zr, **2a**; Hf, **2b**) and Li(THF)$_3$SiPh$_2$Bu^t similarly yielded **4a** or **4b**. The reaction of **2a** with Li(THF)$_3$SiPh$_2$Bu^t was used in the kinetic studies to be discussed below.

For **3a**: ^{1}H NMR (benzene-d_6, 400.0 MHz, 23 °C) δ 3.52, 1.35 (m, THF), 0.55 [s, N(SiMe_3)$_2$]; ^{13}C{^{1}H} NMR (benzene-d_6, 100.6 MHz, 23 °C) δ 68.1, 25.6 (THF), 6.81 [N(SiMe_3)$_2$].

For **3b**: ^{1}H NMR (benzene-d_6, 400.0 MHz, 23 °C) δ 3.44, 1.34 (m, THF), 0.57 [s, N(SiMe_3)$_2$]; ^{13}C{^{1}H} NMR (benzene-d_6, 100.6 MHz, 23 °C) δ 68.2, 25.5 (THF), 6.97 [N(SiMe_3)$_2$].

For **4a**: ^{1}H NMR (benzene-d_6, 400.0 MHz, 23 °C) δ 3.53 (m, 8H, THF), 1.36 (m, 8H, THF), 0.49 [s, 36H, N(SiMe_3)$_2$], 0.31 (s, 9H, NSiMe_3), 0.24 (s, 9H, NSiMe_3); ^{13}C{^{1}H} NMR (benzene-d_6, 100.6 MHz, 23 °C) δ 68.0, 25.6 (THF), 5.88 [N(SiMe_3)$_2$], 5.43 (NSiMe_3), 4.00 (NSiMe_3). FT-IR (Nujol): 2957 (s), 2898 (m), 1247 (s), and 1030 (s) cm^{-1}. Anal. calcd for C$_{26}$H$_{71}$N$_4$Si$_6$O$_2$LiZr: C, 42.28; H, 9.69. Found: C, 41.98; H, 9.65.

For **4b**: ^{1}H NMR (benzene-d_6, 400.0 MHz, 23 °C) δ 3.48 (m, 8H, THF), 1.30 (m, 8H, THF), 0.50 [s, 36H, N(SiMe_3)$_2$], 0.32 (s, 9H, NSiMe_3), 0.23 (s, 9H, NSiMe_3); ^{13}C{^{1}H} NMR (benzene-d_6, 100.6 MHz, 23 °C) δ 68.3, 25.4 (THF), 6.18 (NSiMe_3), 6.07 [N(SiMe_3)$_2$], 3.99 (NSiMe_3). FT-IR (Nujol): 3422 (w), 2953 (s),

(7) Campion, B. K.; Heyn, R. H.; Tilley, T. D. *Organometallics* **1993**, *12*, 2584.
(8) Morse, P. M.; Spencer, M. D.; Wilson, S. R.; Girolami, G. S. *Organometallics* **1994**, *13*, 1646.
(9) See Supporting Information for details.

Table 1. Rate Constants k for the **3a** → **4a** Conversion[a]

T (K)	$(k \pm \delta k_{(ran)}) \times 10^5$ (s^{-1})
290 ± 1	2.36 ± 0.15
295 ± 1	3.55 ± 0.17
300 ± 1	5.1 ± 0.3
305 ± 1	7.6 ± 0.7
310 ± 1	11.5 ± 1.0
315 ± 1	15.8 ± 0.4

[a] The largest random uncertainty is $\delta k_{(ran)}/k = 0.68/7.58 = 9.0\%$. The total uncertainty of $\delta k/k = 10.3\%$ was calculated from $\delta k_{(ran)}/k = 9.0\%$ and estimated systematic uncertainty $\delta k_{(sys)}/k = 5\%$. The total uncertainty $\delta k/k$ and $\delta T = 1$ K were used in the calculations of uncertainties in the activation enthalpy $\Delta H^{\ddagger}$ and activation entropy $\Delta S^{\ddagger}$ by the error propagation formulas derived from the Eyring equation by Girolami and co-workers.[8]

2898 (m), 1252 (s), and 1068 (s) cm^{-1}. Anal. calcd for $C_{26}H_{71}N_4Si_6O_2LiHf$: C, 37.81; H, 8.67. Found: C, 37.68; H, 8.44.

Kinetic Studies of the Conversion of Li(THF)$_n${HN−M[N(SiMe$_3$)$_2$]$_3$} (3a) to Li(THF)$_2${Me$_3$SiN−M[NH(SiMe$_3$)][N(SiMe$_3$)$_2$]$_2$} (4a). Complex **3a** was prepared in situ by mixing $H_2N-Zr[N(SiMe_3)_2]_3$ (**2a**) and $Li(THF)_3SiPh_2Bu^t$ in a ratio of 1.20:1. Since the reaction requires THF,[10] THF (0.600 g) was added to toluene-d_8 (10.0 g) as a mixed solvent used in the kinetic studies. In a typical kinetic study, **2a** (46.9 mg, 20% excess) and $Li(THF)_3SiPh_2Bu^t$ (25.4 mg) were mixed with 4,4′-dimethyl biphenyl (an internal standard) in a Young's NMR tube and the THF/toluene-d_8 mixed solvent was added to give a final volume of 0.567 mL and the THF concentration (C_{THF}) of 1.07 M. The mixture was frozen at −50 °C as soon as the solvents were added. The NMR spectrometer was preset to the temperature, and the NMR tube was briefly thawed shortly before the NMR tube was inserted to the spectrometer. ^{1}H spectra were recorded directly on the NMR spectrometer. Rate constants derived from fitting of the data by first-order kinetics are given in Table 1.

Studies of the Effect of THF on the Rate of the 3a → 4a Conversion. Three mixtures of toluene-d_8 (5.00 g) and THF (0.600, 0.500, and 0.400 g, respectively) were used as solvents for the reactions. In a typical study of the THF effect, $H_2N-Zr[N(SiMe_3)_2]_3$ (**2a**, 49.2 mg, 20% excess) and $Li(THF)_3SiPh_2Bu^t$ (26.6 mg) were mixed with an internal standard 4,4′-dimethyl biphenyl in a Young's NMR tube, and the THF/toluene-d_8 mixed solvent was added to give a final volume of 0.523 mL. The THF concentrations (C_{THF}) of the samples were calculated from THF in the original THF/toluene-d_8 mixed solvent and THF in $Li(THF)_3SiPh_2Bu^t$, and C_{THF} were 1.81, 1.58, and 1.34 M, respectively. The mixture was frozen at −50 °C as soon as THF/toluene-d_8 was added. The NMR spectrometer was preset to 290 K, and the NMR tube was briefly thawed shortly before the NMR tube was inserted to the spectrometer. ^{1}H spectra were recorded directly on the NMR spectrometer. Rate constants derived from fitting of the data by first-order kinetics {rate = k[**3a**], ($k = aC_{THF}^m$)} are given in Table 2.

Results from a prior study at 290 K (Table 1) involving 10.00 g of toluene-d_8 and 0.600 g of THF were used for the current study. The THF concentration of this sample was 1.07 M.

Determination of X-ray Crystal Structures of 2a, 4a, and 4b. The data for the crystal structures of these complexes were collected on a Bruker AXS Smart 1000 X-ray diffractometer (Mo radiation) equipped with a CCD area detector and fitted with an upgraded Nicolet LT-2 low-temperature device. Suitable crystals were coated with paratone oil (Exxon) and mounted on a hairloop under a stream of nitrogen gas at −100(2) °C. All the structures were solved by direct methods. In all cases, the non-hydrogen atoms were refined with anisotropic displacement coefficients. All hydrogen atoms were included in the structure factor calculation at idealized positions and were allowed to ride on the neighboring atoms with relative isotropic displacement coefficients. Empirical absorption correction was performed with SADABS.[11a] All calculations were performed using SHELXTL (Version 5.1) proprietary software package.[11b]

Table 2. Rate Constants k at 290 K for the **3a** → **4a** Conversion with Different C_{THF}[a]

C_{THF} (M)	$(k \pm \delta k_{(ran)}) \times 10^5$ (s^{-1})
1.07	2.36 ± 0.15
1.34	4.2 ± 0.5
1.58	7.9 ± 0.4
1.81	14.1 ± 0.5

[a] The largest random uncertainty is $\delta k_{(ran)}/k = 0.52/4.23 = 12.3\%$. The total uncertainty of $\delta k/k = 13.3\%$ was calculated from $\delta k_{(ran)}/k = 12.3\%$ and estimated systematic uncertainty $\delta k_{(sys)}/k = 5\%$.

Results and Discussion

Synthesis and Characterization of Peramide Zr and Hf Complexes $H_2N-M[N(SiMe_3)_2]_3$ (M = Zr, 2a; Hf, 2b). Chloride ligands in $Cl-M[N(SiMe_3)_2]_3$ (M = Zr, **1a**; Hf, **1b**) are not usually attacked directly by groups larger than methyl mainly because of the bulkiness of $-N(SiMe_3)_2$ ligands in these complexes.[12] NH_3, a molecule similar to $-CH_3$ in size, reacted with **1a** and **1b** to give NH_4Cl and $H_2N-M[N(SiMe_3)_2]_3$ (M = Zr, **2a**; Hf, **2b**), respectively, in ca. 34% yields. Byproducts as white precipitates insoluble in most of the common solvents were also observed. The $-NH_2$ peaks in ^{1}H NMR spectra of **2a**−**b** showed a 1:1:1 triplet at 4.26 ppm with $^1J(^{14}N-H) = 45.6$ Hz for **2a** and at 3.67 ppm with $^1J(^{14}N-H) = 46.0$ Hz for **2b**, respectively. This is significantly downfield shifted from −0.52 ppm [$^1J(^{14}N-H) = 64$ Hz] in {HC[C(Me)N(Ar)]$_2$}Al(NH_2)$_2$[13a] and 2.07 ppm in [(tritox)Zr]$_6$(μ_6-N)(μ_3-NH)$_6$(μ_2-NH_2)$_3$.[3a] It is not clear what leads to the large downfield shift of the $-NH_2$ peak in **2a**. **2a** and **2b** are among the few transition-metal amides with the $-NH_2$ ligands. In the IR spectra of **2a** and **2b**, $-NH_2$ peaks with low intensities were observed at 3342 cm^{-1} for **2a** and 3364 cm^{-1} for **2b**, respectively. In comparison, the following N−H stretching frequencies were reported: 3384 cm^{-1} in K[{(Cp*Zr)$_3$(μ_3-N)(μ_3-NH)(μ_3-NH_2)$_3$}$_4$(NH_2)$_5$(NH_3)$_7$]·6C_7H_8,[3b] 3396 cm^{-1} in {HC[C(Me)N(Ar)]$_2$}Al(NH_2)$_2$,[13a] 3350, 3420 cm^{-1} in [$(CH_3)_2AlNH_2$]$_3$,[13b] and 3317, 3260 cm^{-1} in [$(Bu^t)_2AlNH_2$]$_3$.[13b]

Observation of Li(THF)$_n${HN−M[N(SiMe$_3$)$_2$]$_3$} (M = Zr, 3a; Hf, 3b) and Preparation of Li(THF)$_2${Me$_3$SiN−M[NH(SiMe$_3$)][N(SiMe$_3$)$_2$]$_2$} (M = Zr, 4a; Hf, 4b). Lithium imide complexes containing the Li^+NH^-−M moiety are

(10) It may not be appropriate to call THF a catalyst in the **3a** → **4a** conversion, although the conversion requires THF to proceed. The extent of THF incorporation in **3a** is unknown, and thus it is not clear whether THF is consumed or gained in the **3a** → **4a** conversion.

(11) (a) Sheldrick, G. M. *SADABS, A Program for Empirical Absorption Correction of Area Detector Data*; University of Göttingen: Göttingen, Germany, 2000. (b) Sheldrick, G. M. *SHELXL-97, A Program for the Refinement of Crystal Structures*; University of Göttingen: Göttingen, Germany, 1997.
(12) Andersen, R. A. *Inorg. Chem.* **1979**, *18*, 1724.
(13) (a) Jancik, V.; Pineda, L. W.; Pinkas, J.; Roesky, H. W.; Neculai, D.; Neculai, A. M.; Herbst-Irmer, R. *Angew. Chem., Int. Ed.* **2003**, *43*, 2142. (b) Interrante, L. V.; Sigel, G. A.; Garbauskas, M.; Hejna, C.; Slack, G. A. *Inorg. Chem.* **1989**, *28*, 252.

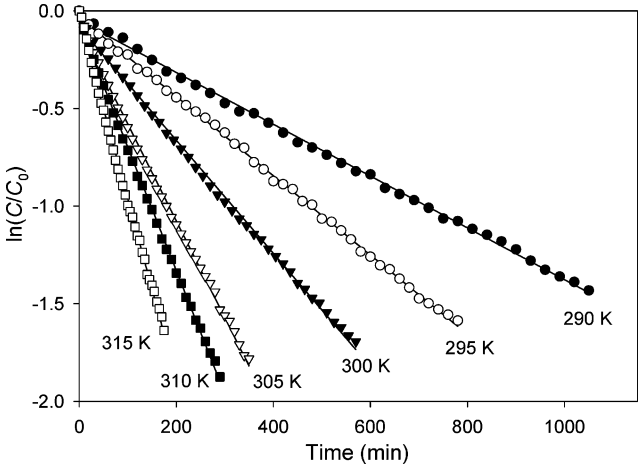

Figure 1. Kinetic plots of the **3a** → **4a** conversion. (C_0 and C are the concentrations of **3a** at $t = 0$ and $t = t$).

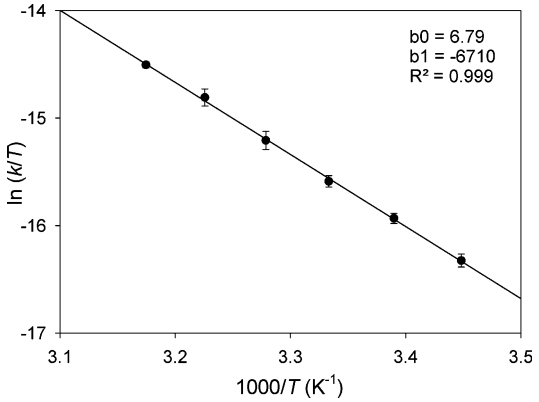

Figure 2. Eyring plot of the **3a** → **4a** conversion.

active reagents for synthesis of metal complexes.[14] Our original plan was to make $Li^+(THF)_n\{HN^-{-}M[N(SiMe_3)_2]_3\}$ (M = Zr, **3a**; Hf, **3b**) from deprotonation of $H_2N{-}M[N(SiMe_3)_2]_3$ (M = Zr, **2a**; Hf, **2b**) by base $Li(THF)_3SiPh_2Bu^t$ or $LiN(SiMe_3)_2$ (Scheme 1), and to use **3a**−**b** as synthetic reagents. The deprotonation reactions did yield **3a** and **3b**.

Complexes **3a** and **3b** were found unstable as solid or in solutions. They underwent the $-SiMe_3$ migration from the $-N(SiMe_3)_2$ to imide ═NH ligands to give $Li^+(THF)_2\{Me_3Si{-}N^-{-}M[NH(SiMe_3)][N(SiMe_3)_2]_2\}$ (M = Zr, **4a**; Hf, **4b**) (Scheme 1).

Kinetic Studies of the 3a → 4a Conversion. The **3a** → **4a** conversion followed first-order kinetics with respect to **3a**. The kinetic studies were conducted between 290 and 315 K in toluene-d_8 containing THF (C_{THF} = 1.07 M) to give plots of ln (C_0/C) (C: concentration of **3a** generated in situ) versus time (Figure 1) and first-order rate constants k of the conversion (Table 1). An Eyring plot (Figure 2) gives activation parameters of the **3a** → **4a** conversion: $\Delta H^‡$ = 13.3(1.3) kcal/mol and $\Delta S^‡ = -34(3)$ eu in THF/toluene-d_8

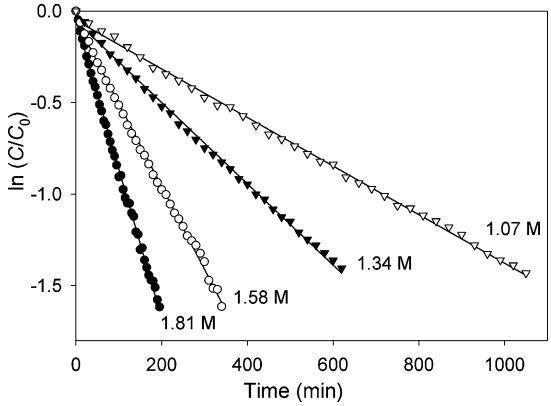

Figure 3. Kinetic plots of the **3a** → **4a** conversion with different C_{THF}.

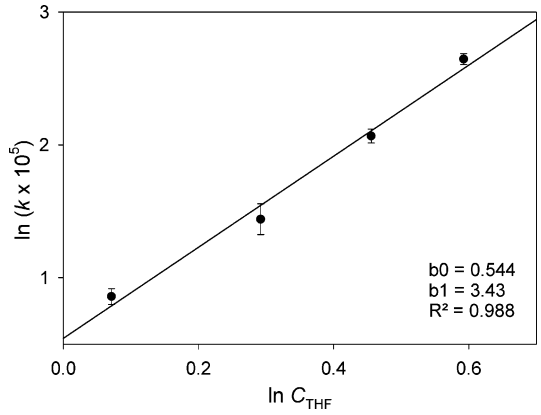

Figure 4. ln ($k \times 10^5$) vs ln C_{THF} plot of the **3a** → **4a** conversion with different THF concentrations.

(C_{THF} = 1.07 M). The activation entropy $\Delta S^‡$ is large and negative, and this issue is discussed below.

THF promoted this conversion.[10] The kinetics of the $-SiMe_3$ migration in the **3a** → **4a** conversion was affected by the concentration of THF in the toluene-d_8 solution. Studies were conducted at 290 K to establish the order of rate constants k with respect to THF (initial concentration of **3a** at 0.115 M; C_{THF} = 1.81, 1.58, 1.34, and 1.07 M, respectively). The plot of ln ($k \times 10^5$) versus ln C_{THF} (Figure 4) gave a slope of 3.4(0.6). The kinetic law for the **3a** → **4a** conversion is given in eqs 2−3.[15]

$$\text{rate} = k\,[\mathbf{3a}];\ k = a[\mathbf{THF}]^{3.4(0.6)} = aC_{THF}^{\ 3.4(0.6)} \qquad (2)$$

$$\ln k = m \ln C_{THF} = 3.4(0.6) \ln C_{THF} \qquad (3)$$

Mechanistic Considerations of the 3a → 4a Conversion. The kinetic studies suggest that THF molecules are involved in the rate-determining step of the reaction. A proposed mechanistic pathway for the **3a**/**3b** → **4a**/**4b** conversions is given in Scheme 2.[6a] THF molecules coordinate to $Li^+(THF)_n$ ions that are partially bonded to the ═N^-H ligand to give perhaps $Li^+(THF)_4$, freeing electron pairs of the ═N^-H ligand. The newly generated imide ═N^-H ligand in **3a**/**3b** then attacks intramolecularly a Si atom in a $-SiMe_3$ group

(14) (a) Lappert, M. F.; Power, P. P.; Sanger, A. R.; Srivastava, R. C. *Metal and Metalloid Amides, Syntheses, Structures, and Physical and Chemical Properties;* Wiley: New York, 1980. (b) Neumann, C.; Schulz, A.; Seifert, T.; Storch, W.; Vosteen, M. *Eur. J. Inorg. Chem.* **2002**, *5*, 1040. (c) Juza, R.; Opp, K. *Z. Anorg. Allg. Chem.* **1951**, *266*, 313. (d) Armstrong, D. R.; Barr, D.; Snaith, R. *Angew. Chem., Int. Ed.* **1991**, *30*, 1707.

(15) Hill, J. W.; Petrucci, R. H. In *General Chemistry, an Integrated Approach*, 3rd ed.; Prentice-Hall: New Jersey, 2002; Chapter 13, pp 553−598.

Scheme 2. Proposed Mechanism of the **3a/3b** → **4a/4b** Conversions

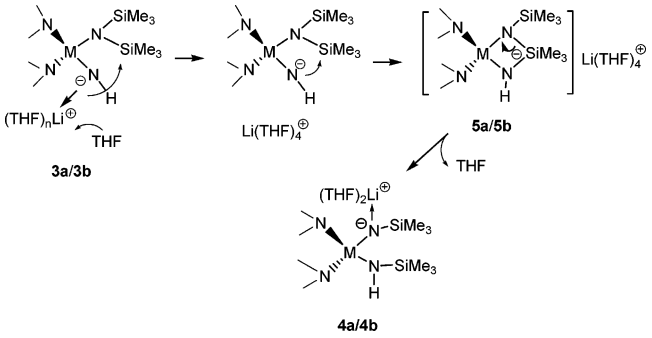

Table 3. Crystal Data for **2**, **4a**, and **4b**

	2	**4a**	**4b**
formula	$C_{18}H_{58}N_4Si_6Zr$	$C_{26}H_{71}LiN_4O_2Si_6Zr$	$C_{26}H_{71}LiN_4O_2Si_6Hf$
fw	590.44	738.57	825.84
temp (°C)	−100(2)	−100(2)	−100(2)
crystal system	hexagonal	triclinic	orthorhombic
space group	*R*3c	$P\bar{1}$	$P2_12_12_1$
a (Å)	18.250(8)	11.666(5)	12.946(5)
b (Å)	18.250(8)	12.283(5)	19.674(7)
c (Å)	17.100(12)	33.923(15)	33.694(12)
α (deg)	90	84.513(7)	90
β (deg)	90	85.172(8)	90
γ (deg)	120	62.462(7)	90
volume (Å^3)	4932(5)	4286(3)	8581(5)
Z	6	4	8
D (cal) (g/cm^3)	1.193	1.145	1.278
μ (mm^{-1})	0.566	0.450	2.624
F(000)	1908	1592	3440
θ range (deg)	2.23−28.23	1.21−28.33	1.20−28.34
completeness (%)	99.6	93.8	98.3
no. of unique reflns	2673	20081	20753
no. of params varied	94	763	763
R indices[a](R_wF^2)	0.0282(0.0314)	0.0424(0.0619)	0.0340(0.0452)
goodness-of-fit on F^2	0.964	0.836	0.978

[a] $R = \sum ||F_o| - |F_c||/\sum|F_o|$; $R_w = (\sum[w(F_o^2 - F_c^2)^2]/\sum[w(F_o^2)^2])^{1/2}$

[of a $-N(SiMe_3)_2$ ligand] to give the intermediate **5a**/**5b** containing a five-coordinate Si atom. This silyl migration yields the amide $-NH(SiMe_3)$ and new imide $=N^--SiMe_3$ ligand in **4a**/**4b** which donate a lone pair of electrons to give $Li^+(THF)_2$, thus regenerating THF. Without the added THF, the THF molecules that were in $Li(THF)_3SiPh_2Bu^t$ very slowly promoted the **3a** → **4a** conversion.[10] The 3.4(0.6)th order of the reaction with respect to THF is also consistent with the large negative activation entropy [$\Delta S^‡ = -34(3)$ eu] of the **3a** → **4a** conversion. $Li(THF)_3SiPh_2Bu^t$ used in the kinetic studies already has three THF per Li^+ ion. A possible multishell of THF molecules around Li^+ cations could be formed at the transition state. In other words, four THF molecules likely coordinate directly to each Li^+ cation. However, additional THF molecules are needed to form outer solvent shells around $Li^+(THF)_4$ ions. This may explain the 3.4(0.6)th order of the reaction with respect to THF. A similar seventh-order reaction with respect to THF was reported by Collum and co-worker in the N-alkylation of lithium diphenylamide by *n*-butyl bromide.[16]

Molecular Structures of 2a, 4a, and 4b. X-ray crystallographic data of **2a**, **4a**, and **4b** are listed in Table 3. A molecular drawing and selected bond distances and angles of $H_2N-Zr[N(SiMe_3)_2]_3$ (**2a**) are given in Figure 5 and Table

(16) Depue, J. S.; Collum, D. B. *J. Am. Chem. Soc.* **1988**, *110*, 5524.

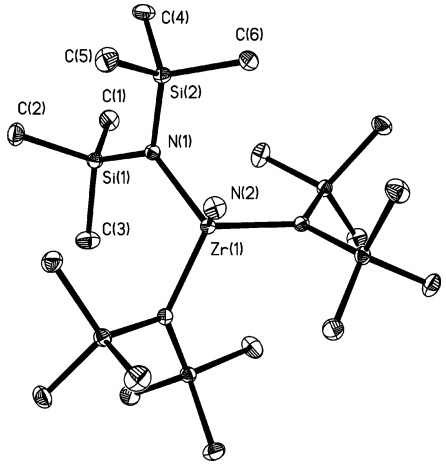

Figure 5. A molecular drawing of **2a** showing 30% probability thermal ellipsoids.

Table 4. Selected Bond Distances (Å) and Angles (°) in **2a**

	distances		
Zr(1)−N(1)	2.097(3)	N(1)−Si(2)	1.764(3)
Zr(1)−N(2)	2.041(6)	C(1)−Si(1)	1.868(4)
N(1)−Si(1)	1.758(3)		
	angles		
N(2)−Zr(1)−N(1)	103.96(7)	Si(1)−N(1)−Zr(1)	126.52(13)
N(1)−Zr(1)−N(1A)	114.38(5)	Si(2)−N(1)−Zr(1)	115.62(13)

4, respectively. **2a** is in the same space group (*R*3c) and crystal system (hexagonal) as its precursor $Cl-Zr[N(SiMe_3)_2]_3$ (**1a**)[17] with similar unit cell parameters [$a = b =$ 18.250(8) Å, $c = 17.100(12)$ Å for **2a** and $a = b = 18.317(3)$ Å, $c = 17.078(4)$ Å for **1a**]. However, $Zr-NH_2$ bond distance of 2.041(6) Å in **2a** is significantly shorter than 2.394(2) Å for Zr−Cl in **1a**. The Zr−N bond distances of $-NH_2$ and $-N(SiMe_3)_2$ ligands are close: 2.041(6) Å for $Zr-NH_2$ and 2.097(3) Å for $Zr-N(SiMe_3)_2$. The N−Zr−N angle between the $-NH_2$ and $-N(SiMe_3)_2$ ligands of 103.96(7)° [N(1)−Zr−N(2)] is smaller than the ideal tetrahedral angle of 109°, perhaps as a result of steric repulsion among the three bulkier $-N(SiMe_3)_2$ ligands. An unsymmetrical alignment of the $-N(SiMe_3)_2$ ligand with respect to the M−N bonds was observed, suggesting the presence of agostic $Si_\beta-C_\gamma$ interaction in **2a**.[18] The Zr(1)···C(6) and Zr(1)···Si(2) distances of 3.53 and 3.27 Å are shorter than those of Zr(1)···C(3) (3.69 Å) and Zr(1)−Si(1) (3.45 Å). The Si(2)−N(1)−Zr(1) bond angles of 115.62(13)° is significantly smaller than that of Si(1)−N(1)−Zr(1) [126.52(13)°], even though the N(1)−Si(1)−C(3) bond angle of 111.22(15)° is similar to that of N(1)−Si(2)−C(6) [111.31(15)°].

Molecular drawings of **4a** and **4b** are given in Figure 6 and Supporting Information,[9] respectively. Selected bond

(17) Airoldi, C.; Bradley, D. C.; Chudzynska, H.; Hursthouse, M. B.; Abdul Malik, K. M.; Raithby, P. R. *J. Chem. Soc., Dalton Trans.* **1980**, 2010.

(18) (a) Koga, N.; Morokuma, K. *J. Am. Chem. Soc.* **1988**, *110*, 108. (b) Eisch, J. J.; Piotrowski, A. M.; Brownstein, S. K.; Gabe, E. J.; Lee, F. L. *J. Am. Chem. Soc.* **1985**, *107*, 7219. (c) Jeske, G.; Schock, L. E.; Swepston, P. N.; Schumann, H.; Marks, T. J. *J. Am. Chem. Soc.* **1985**, *107*, 8103. (d) Den Haan, K. H.; De Boer, J. L.; Teuben, J. H.; Spek, A. L.; Kojic-Prodic, B.; Hays, G. R.; Huis, R. *Organometallics* **1986**, *5*, 1726.

Table 5. Selected Bond Distances (Å) and Angles (°) in **4a**−**b**

distances					
	4a (M = Zr)	**4b** (M = Hf)		**4a**	**4b**
M(1)−N(1)	2.146(3)	2.124(5)	N(1)−Si(1)	1.744(3)	1.741(5)
M(1)−N(2)	2.163(2)	2.140(5)	N(3)−Si(5)	1.741(3)	1.724(5)
M(1)−N(3)	2.142(3)	2.094(5)	N(4)−Si(6)	1.703(3)	1.721(5)
M(1)−N(4)	1.911(3)	1.906(5)	Li(1)−O(1)	2.061(6)	2.010(12)
Li(1)−N(3)	2.201(6)	2.257(11)	Li(1)−O(2)	2.003(6)	1.996(11)
Li(1)−N(4)	2.122(6)	2.058(12)	C(1)−Si(1)	1.866(4)	1.885(8)
angles					
	4a	**4b**		**4a**	**4b**
N(1)−M(1)−N(2)	120.75(9)	118.34(18)	N(4)−Li(1)−N(3)	88.6(2)	87.9(4)
N(1)−M(1)−N(3)	108.63(9)	108.17(19)	Si(5)−N(3)−M(1)	135.92(14)	138.0(3)
N(2)−M(1)−N(3)	109.25(10)	108.4(2)	Si(6)−N(4)−M(1)	155.28(17)	156.8(3)
N(1)−M(1)−N(4)	109.88(10)	111.5(2)	Si(5)−N(3)−Li(1)	117.03(19)	119.0(4)
N(2)−M(1)−N(4)	109.43(10)	111.2(2)	Si(6)−N(4)−Li(1)	108.7(2)	109.0(4)
N(3)−M(1)−N(4)	96.09(11)	97.0(2)	Si(3)−N(2)−M(1)	117.17(13)	115.7(3)
M(1)−N(3)−Li(1)	83.66(17)	82.2(3)	Si(4)−N(2)−M(1)	122.36(13)	123.9(3)
M(1)−N(4)−Li(1)	91.67(19)	92.4(3)			

distances and angles of **4a**−**b** are listed in Table 5. Both structures of **4a** and its Hf analogue **4b**, which are similar but not isomorphous, contain two independent molecules with similar structures. The structure of **4a** is discussed below. The crystal structure of **4a** showed distorted tetrahedral Zr and Li metal centers. The cycle defined by Zr(1)−N(4)−Li(1)−N(3) is almost coplanar. The Zr(1)−N(4) bond distance of 1.911(3) Å for the Zr−N^{-}−SiMe$_3$ imide ligand is shorter than those of amides [Zr(1)−N(3) of 2.142(3), Zr(1)−N(2) of 2.163(2), and Zr(1)−N(1) of 2.146(3) Å]. The Si(6) atom in the Zr−N^{-}−SiMe$_3$ moiety is nearly in the plan defined by Zr(1)−N(4)−Li(1)−N(3) as a result of the N(4) partial sp^2 hybridization. The Zr(1)···C(6) and Zr(1)···Si(2) distances of 3.35 and 3.31 Å are significantly shorter than Zr(1)···C(1) (3.85 Å) and Zr(1)···Si(1) (3.45 Å) distances, respectively. The Si(2)−N(1)−Zr(1) and N(1)−Si(2)−C(6) bond angles of 116.70(12) and 110.16(14)° are smaller than those of Si(1)−N(1)−Zr(1) [124.37(13)°] and N(1)−Si(1)−C(1) [112.45(14)°]. These observations suggest agostic Si$_\beta$−C$_\gamma$ interaction[18] between Zr(1) and the Zr(1)−N(1)−Si(2)−C(6) moiety. The Zr(1)···C(7) and Zr(1)···Si(3) distances of 3.33 and 3.33 Å are shorter than Zr(1)···C(12) (3.96 Å) and Zr(1)···Si(4) (3.41 Å) distances, respectively. The Si(3)−N(2)−Zr(1) and N(2)−Si(3)−C(7) bond angles of 117.17(13) and 108.95(14)° are smaller than those of Si(4)−N(2)−Zr(1) [122.36(13)°] and N(2)−Si(4)−C(12) [112.29(15)°]. These observations also suggest agostic Si$_\beta$−C$_\gamma$ interaction between Zr(1) and the Zr(1)−N(2)−Si(3)−C(7) moiety.

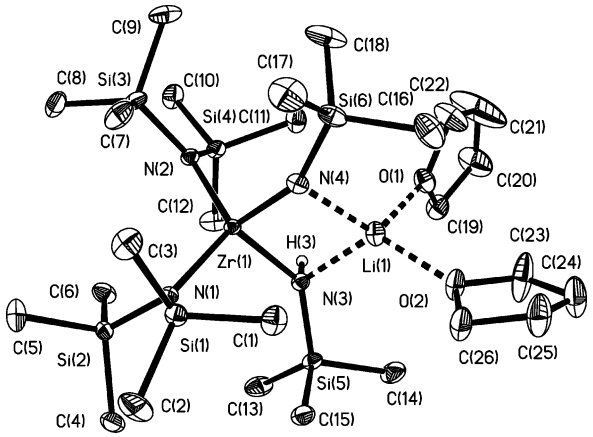

Figure 6. A molecular drawing of **4a** showing 30% probability thermal ellipsoids.

Acknowledgment. Acknowledgment is made to the National Science Foundation (CHE-0212137) and the Ziegler Research Fund for financial support of the research. The authors thank Prof. David B. Collum and reviewers for helpful suggestions.

Supporting Information Available: Derivation of the error propagation formula for σm, molecular drawing of **4b**, and crystallographic data for **2**, **4a**, and **4b**. This material is available free of charge via the Internet at http://pubs.acs.org.

IC0485413